

Hindawi Publishing Corporation  
Journal of Nanomaterials  
Volume 2016, Article ID 2131940, 6 pages  
<http://dx.doi.org/10.1155/2016/2131940>



## Research Article

# Magnetic and Electrical Properties of Heusler Alloy $\text{Co}_2\text{MnSi}$ Thin Films Grown on $\text{Ge}(001)$ Substrates via an $\text{Al}_2\text{O}_3$ Tunnel Barrier

Gui-fang Li, Shibin Liu, and Yongqian Du

School of Electronics and Information, Northwestern Polytechnical University, 127 West Youyi Road, Xi'an, Shaanxi 710072, China

Correspondence should be addressed to Gui-fang Li; [gfli@nwpu.edu.cn](mailto:gfli@nwpu.edu.cn)

Received 4 September 2015; Revised 27 November 2015; Accepted 10 December 2015

Academic Editor: Oscar Perales-Pérez

Copyright © 2016 Gui-fang Li et al. This is an open access article distributed under the Creative Commons Attribution License, which permits unrestricted use, distribution, and reproduction in any medium, provided the original work is properly cited.

Heusler alloy  $\text{Co}_2\text{MnSi}/\text{Al}_2\text{O}_3$  heterostructures on single-crystal  $\text{Ge}(001)$  substrates were prepared through magnetron sputtering for both  $\text{Co}_2\text{MnSi}$  and  $\text{Al}_2\text{O}_3$  thin films as a promising candidate for future-generation semiconductor-based spintronic devices. Sufficiently high saturation magnetization  $781 \text{ emu/cm}^3$  was obtained for the  $\text{Co}_2\text{MnSi}$  thin film. Furthermore, the current versus voltage ( $I$ - $V$ ) characteristics showed that the tunneling conduction was dominant in  $\text{Co}_2\text{MnSi}/\text{Al}_2\text{O}_3$  (2 nm)/ $\text{Ge}(001)$  heterostructure and the  $I$ - $V$  characteristics were slightly dependent on temperature. The conductance versus voltage ( $dI/dV$ - $V$ ) characteristics indicated that the potential barrier height at the  $\text{Co}_2\text{MnSi}/\text{Al}_2\text{O}_3$  interface was almost equal to that at the  $n$ - $\text{Ge}/\text{Al}_2\text{O}_3$  interface for the prepared  $\text{Co}_2\text{MnSi}/\text{Al}_2\text{O}_3/\text{Ge}(001)$  heterostructure.

## 1. Introduction

Injection and manipulation of spin-polarized electrons in semiconductor channels to create viable semiconductor-based spintronic devices has attracted increasing interests in recent years [1–3]. Spin injection from a ferromagnetic electrode into semiconductor channel via a Schottky tunnel barrier or an insulating tunnel barrier has been extensively studied [4–6]. To realize the highly efficient spin injection from ferromagnetic electrode into semiconductor channel, the highly polarized spin injection source and high mobility semiconductor channel are indispensable. Heusler alloy  $\text{Co}_2\text{MnSi}$  is one of the most promising candidates for spin injection into semiconductor channel due to the theoretically predicted 100% spin polarization [7, 8]. It has been shown that the giant tunnel magnetoresistance (TMR) ratios of 354% at 290 K and 1995% at 4.2 K were observed for fully epitaxial  $\text{Co}_2\text{MnSi}/\text{MgO}/\text{Co}_2\text{MnSi}$  magnetic tunneling junctions (MTJs) on  $\text{CoFe}$ -buffered  $\text{MgO}$  substrate [9]. Germanium (Ge), which owns the high mobility of electrons and holes, is an excellent candidate for next generation semiconductor channel materials of metal-oxide-semiconductor devices. Therefore, the combination of Heusler alloy  $\text{Co}_2\text{MnSi}$  and

Ge has great potential for highly efficient spin injection into Ge channel. Moreover, in order to solve the lattice mismatch problem between the ferromagnetic metal and Ge channel, an insulator layer was always inserted between them [10–12]. In such kind of metal/insulator/semiconductor (M/I/SC) heterostructure, previous studies have reported that the magnitude of the observed spin signal was several orders larger than the magnitude from what is expected based on the available theory for spin injection and diffusion [12–14]; importantly, the spin signal varied with the thickness of the tunnel barrier [15, 16]. At present, the physical mechanism for the anomalous scaling of the spin signal was still unclear. Thus, it is important to fabricate various heterostructures with high quality insulator tunnel barriers. In our previous study, the  $\text{Co}_2\text{MnSi}$  thin film was directly grown on  $\text{Ge}(001)$  substrate due to the relatively small lattice mismatch (less than 1%) between the  $\text{Co}_2\text{MnSi}$  and  $\text{Ge}(001)$ . In order to obtain the high quality  $\text{Co}_2\text{MnSi}$  film,  $\text{Co}_2\text{MnSi}/\text{Ge}$  heterostructure was *in situ* annealed at temperature above  $300^\circ\text{C}$ , but the interdiffusion between the  $\text{Co}_2\text{MnSi}$  and  $\text{Ge}(001)$  becomes a serious problem. Thus, an insulator layer was needed to be inserted between Heusler alloy and Ge channel. Then, in further study, Heusler alloy  $\text{Co}_2\text{MnSi}$  thin

film was epitaxially grown on the Ge(001) single-crystal via MgO tunnel barrier through magnetron sputtering for the Co<sub>2</sub>MnSi and electron beam evaporation for the MgO [17]. However, there are rare reports on fabrication of Co<sub>2</sub>MnSi thin film grown on Ge channel via high quality Al<sub>2</sub>O<sub>3</sub> tunnel barrier and investigation of electrical properties of the Co<sub>2</sub>MnSi/Al<sub>2</sub>O<sub>3</sub>/Ge(001) heterostructure.

Our purpose in the present study has been to fabricate Heusler alloy Co<sub>2</sub>MnSi thin films on Ge(001) substrates via an Al<sub>2</sub>O<sub>3</sub> tunnel barrier and to investigate their magnetic and electrical properties. We firstly prepared 20 nm thick Co<sub>2</sub>MnSi thin film on the Ge(001) substrate via an Al<sub>2</sub>O<sub>3</sub> tunnel barrier, and both the Co<sub>2</sub>MnSi thin film and the Al<sub>2</sub>O<sub>3</sub> tunnel barrier were prepared by magnetron sputtering. A high saturation magnetization of 781 emu/cm<sup>3</sup> was obtained for the Co<sub>2</sub>MnSi thin film grown on Ge(001) substrate with annealing temperature  $T_a = 500^\circ\text{C}$ . Furthermore, the barrier thickness calculated from the current- ( $I$ -) voltage ( $V$ ) characteristics of Co<sub>2</sub>MnSi/Al<sub>2</sub>O<sub>3</sub>/Ge(001) heterostructure was close to the nominal thickness of the deposited Al<sub>2</sub>O<sub>3</sub>, which indicated that the Al<sub>2</sub>O<sub>3</sub> layer works effectively as a tunnel barrier. These results demonstrated that Co<sub>2</sub>MnSi/Al<sub>2</sub>O<sub>3</sub> heterostructure was promising for efficient spin injection into a semiconductor channel of the Ge featuring high mobility.

This paper is organized as follows. Section 2 describes experimental methods. Section 3 presents our experimental results regarding magnetic properties and electrical properties of Co<sub>2</sub>MnSi/Al<sub>2</sub>O<sub>3</sub>/Ge(001) heterostructure and discussion. Section 4 summarizes our results and concludes.

## 2. Experimental Methods

We describe the preparation of Co<sub>2</sub>MnSi/Al<sub>2</sub>O<sub>3</sub>/ $n$ -Ge heterostructures and their characterization methods.  $n$ -type Ge(001) substrates were used (carrier concentration  $n_1 = 4.0 \times 10^{14} \text{ cm}^{-3}$ , specific resistance  $\rho = 22 \Omega \text{ cm}$ ). Phosphorus ions were implanted with an input dosage of  $5 \times 10^{14} \text{ cm}^{-2}$  (50 keV). For surface cleaning, the ion-implanted substrate surface was intentionally oxidized at  $550^\circ\text{C}$  for 5 min in a furnace with an oxygen gas flow, and the sacrificed oxidation layer was removed with hydrofluoric acid solution. For the preparation of Co<sub>2</sub>MnSi/Al<sub>2</sub>O<sub>3</sub>/ $n$ -Ge heterostructures, we decreased the oxidation time of the ion-implanted Ge substrates to 5 min to make the thickness of the oxidized surface layer sufficiently lower than the  $n$ -type channel thickness of about 100 nm ( $n_2 = 5.4 \times 10^{18} \text{ cm}^{-3}$  at 290 K). The Ge substrate was then annealed for further surface cleaning in the ultrahigh vacuum chamber with base pressure of  $5.0 \times 10^{-4}$ . For this annealing process, we increased the substrate temperature ( $T_s$ ) to a certain temperature near  $500^\circ\text{C}$  for 5 min and then decreased  $T_s$  to room temperature (RT). All layers in the heterostructure consisting of (from the upper side) Ru cap (5 nm)/Co<sub>2</sub>MnSi (20 nm)/Al<sub>2</sub>O<sub>3</sub> barrier (2 nm) grown on a  $n$ -type Ge substrate were successively deposited in an ultrathin vacuum chamber through the magnetron sputtering for the Co<sub>2</sub>MnSi and Al<sub>2</sub>O<sub>3</sub> thin films.

The magnetic properties of Co<sub>2</sub>MnSi thin films were investigated with vibrating sample magnetometer (VersaLab,

Quantum Design) at RT. The junctions with sizes ranging from  $30 \times 30 \mu\text{m}^2$  to  $150 \times 150 \mu\text{m}^2$  were fabricated. The current versus voltage ( $I$ - $V$ ) characteristics and conductance versus voltage ( $dI/dV$ - $V$ ) characteristics for each junction were measured at 290 K using a three-terminal geometry.

## 3. Results and Discussion

**3.1. Magnetic Properties of 20 nm Thick Thin Films Grown on Ge(001) Substrates via an Al<sub>2</sub>O<sub>3</sub> Tunnel Barrier.** First, we describe the magnetic properties of 20 nm thick Co<sub>2</sub>MnSi films on Al<sub>2</sub>O<sub>3</sub> tunnel barrier (2 nm)/Ge(001) substrates. Figure 1(a) shows typical magnetic hysteresis curves at 290 K for Co<sub>2</sub>MnSi films after deposition annealed with temperature ranging from  $400^\circ\text{C}$  to  $500^\circ\text{C}$ , where the magnetic field was applied in the plane of the film. With increasing  $T_a$  from  $400$  to  $500^\circ\text{C}$ , the saturation magnetization ( $M_s$ ) increased. The increase of  $M_s$  was probably related to the improvement of the crystalline structure of the Co<sub>2</sub>MnSi thin films with increase of the annealing temperature according to our previous study [17]. In order to confirm this supposition, the X-ray diffraction measurement was done to investigate the typical peaks of Co<sub>2</sub>MnSi thin films by  $\theta$ - $2\theta$  scan. No reliable results were obtained, which may be due to the overlapped diffraction peaks of the Co<sub>2</sub>MnSi and Ge(001) substrates. In fact, the Bragg diffraction angles for any diffraction peaks for Co<sub>2</sub>MnSi and Ge are almost equal due to the small lattice constants difference.

With continuous increasing  $T_a$  up to  $550^\circ\text{C}$ , no appreciable magnetic hysteresis curve was observed for Co<sub>2</sub>MnSi/Al<sub>2</sub>O<sub>3</sub>/Ge(001) heterostructure (not shown in Figure 1(a)), which was probably due to the unnegligible interdiffusion between the Co<sub>2</sub>MnSi thin film and the Ge(001) substrate. Indeed, the surface of the sample became bad when the annealing temperature increased up to  $550^\circ\text{C}$ , indicating that a serious interdiffusion occurred.

Figure 1(b) shows  $M_s$  values as a function of  $T_a$  at 290 K for Co<sub>2</sub>MnSi films. The  $M_s$  values at 290 K increased with increasing  $T_a$  from  $M_s = 622 \text{ emu/cm}^3$  for  $T_a = 400^\circ\text{C}$  to  $M_s = 722 \text{ emu/cm}^3$  for  $T_a = 450^\circ\text{C}$ . With continuous increasing temperature up to  $500^\circ\text{C}$ , the  $M_s$  value slightly increased up to  $781 \text{ emu/cm}^3$ . The maximum saturation magnetization  $781 \text{ emu/cm}^3$  was in good agreement with the  $859 \text{ emu/cm}^3$  for Co<sub>2</sub>MnSi thin film grown on a MgO-buffered MgO substrate [18], which indicates that the prepared Co<sub>2</sub>MnSi thin film possessed comparable magnetization value to the Co<sub>2</sub>MnSi grown on MgO-buffered MgO substrate

**3.2. Electrical Properties of Co<sub>2</sub>MnSi/Al<sub>2</sub>O<sub>3</sub>/Ge Heterostructures.** Next, we describe  $I$ - $V$  characteristics of the prepared junctions measured with a three-terminal geometry. Figure 2(a) shows a schematic diagram of the device structure and the three-terminal circuit geometry for measuring  $I$ - $V$  characteristics. The bias voltage is applied between terminal 2 and terminal 1. The voltage across the junction 2 was obtained by measurement of the voltage between terminals 2 and 3. In addition, the current across the junction 2 was measured by the current meter between terminal 2

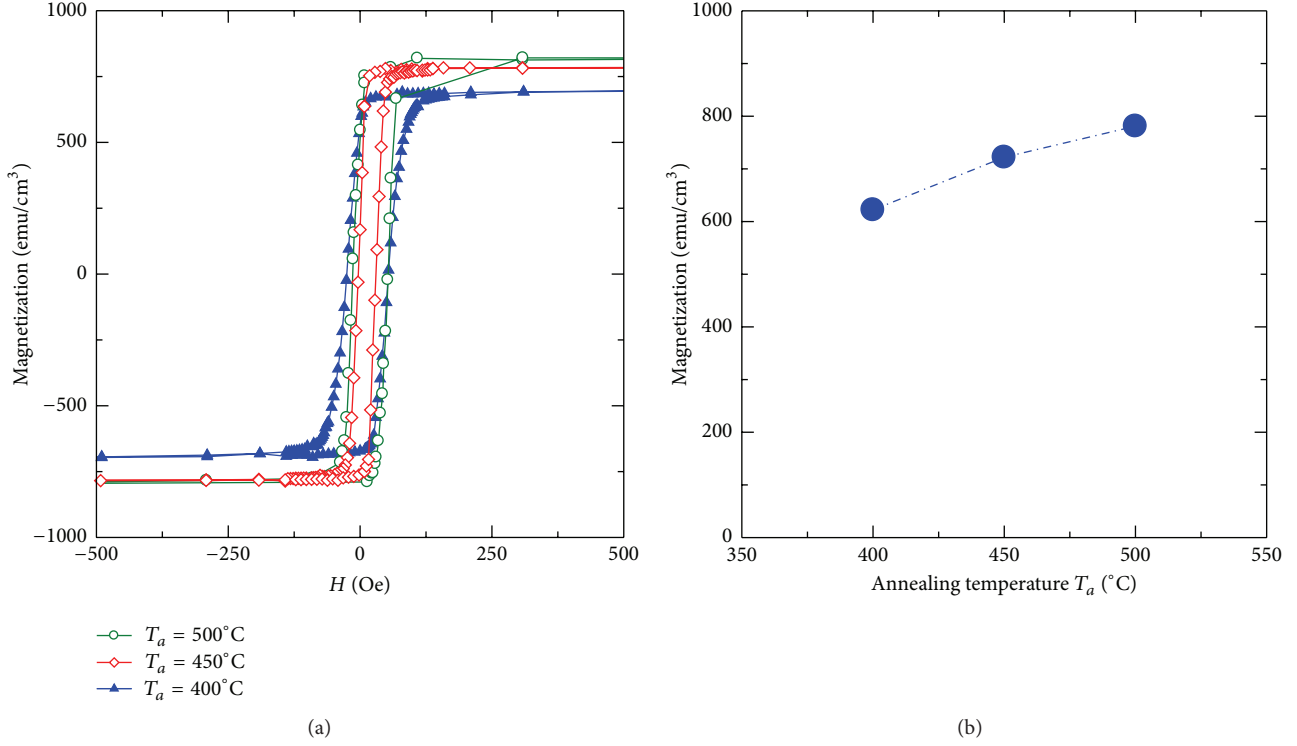


FIGURE 1: (a) Typical magnetic hysteresis curves at 290 K for  $\text{Co}_2\text{MnSi}$  films after deposition annealed with temperature ranging from 400°C to 500°C, where the magnetic field was applied in the plane of the film. (b)  $M_s$  values as a function of  $T_a$  at 290 K for  $\text{Co}_2\text{MnSi}$  films.

and terminal 1. For negative (positive) bias, the metal (M)/insulator (I)/semiconductor (SC) (M/I/SC) junction is reverse-biased (forward-bias).

Figure 2(b) shows typical  $I$ - $V$  characteristics of a  $\text{Co}_2\text{MnSi}/\text{Al}_2\text{O}_3/n\text{-Ge}$  junction with a junction area of  $60 \times 60 \mu\text{m}^2$ . The  $I$ - $V$  characteristics showed nonlinear characteristics and were almost symmetric with respect to the bias polarity, which indicated that the tunneling conduction was dominant. However, a slightly larger current was obtained for the forward bias, which was probably due to a thermionic emission current through the  $\text{Al}_2\text{O}_3/n\text{-Ge}$  interface for the forward bias.

In order to estimate the potential barrier height and tunnel barrier thickness, the  $I$ - $V$  curve was fitted based on Simmons's formula which is expressed as follows [19]:

$$J = \left( \frac{e^2}{\hbar} \right) \frac{\sqrt{2m^* \varphi_0}}{\hbar} \frac{1}{d} \exp(-\gamma) (V + \beta V^3), \quad (1)$$

$$\beta = \gamma \left( \frac{\gamma}{96} - \frac{1}{32} \right) \left( \frac{e}{\varphi_0} \right)^2, \quad (2)$$

$$\gamma = \frac{4\pi d}{\hbar} \sqrt{2m^* \varphi_0}, \quad (3)$$

where  $J$  is density of current,  $\hbar$  is the Plank constant,  $m^*$  is the effective electron mass normalized by the bare electron mass,  $\varphi_0$  is the averaged potential barrier height (the energy difference between the Fermi level of the  $\text{Co}_2\text{MnSi}$  and

the bottom of the conduction band of the  $\text{Al}_2\text{O}_3$  tunnel barrier),  $d$  is tunnel barrier thickness, and  $V$  is applied voltage. Figure 2(b) shows the fitted  $I$ - $V$  curve based on (1), and we estimated the potential barrier height  $\varphi_0$  in the form of  $m^* \varphi_0$  for  $\text{Co}_2\text{MnSi}/\text{Al}_2\text{O}_3/\text{Ge}$  heterostructure as  $m^* \varphi_0 = 0.38 \text{ eV}$  and  $d = 1.9 \text{ nm}$ . The calculated value of  $d$  was close to the nominal thickness of the deposited  $\text{Al}_2\text{O}_3$ , indicating that the  $\text{Al}_2\text{O}_3$  layer acts effectively as a tunnel barrier.

Figure 3(a) shows the  $I$ - $V$  characteristics at various temperatures ( $T$ ) measured by three-terminal geometry. The  $I$ - $V$  curves showed nonlinear characteristics and all of them are almost symmetric with bias. The  $I$ - $V$  characteristics were slightly dependent on temperature. Figure 3(b) shows the ratios of the resistance at  $T$  and 290 K for a DC current of  $0.5 \mu\text{A}$ . We found that  $R(T)/R(290 \text{ K})$  shows a weak dependence on the temperature, which is as expected for tunneling characteristics [20]. This proves that the tunneling process through the  $\text{Al}_2\text{O}_3$  barrier is dominant for the transport.

Figure 4 shows typical conductance versus voltage ( $dI/dV$ - $V$ ) characteristics at 290 K for the  $\text{Co}_2\text{MnSi}/\text{Al}_2\text{O}_3$  (2.0 nm)/ $n\text{-Ge}$  heterostructure. The conductance took the minimum value at a relatively low bias voltage of 12 mV, indicating that the potential barrier height at the  $\text{Co}_2\text{MnSi}/\text{Al}_2\text{O}_3$  interface (the energy difference between the bottom of the conduction band of the  $\text{Al}_2\text{O}_3$  tunnel barrier and the Fermi level of the  $\text{Co}_2\text{MnSi}$ ) was almost equal to that at the  $n\text{-Ge}/\text{Al}_2\text{O}_3$  interface (the energy difference between the bottom of the conduction band of the  $\text{Al}_2\text{O}_3$  tunnel barrier and the Fermi level of the  $n\text{-Ge}$ ). With increasing the bias voltage

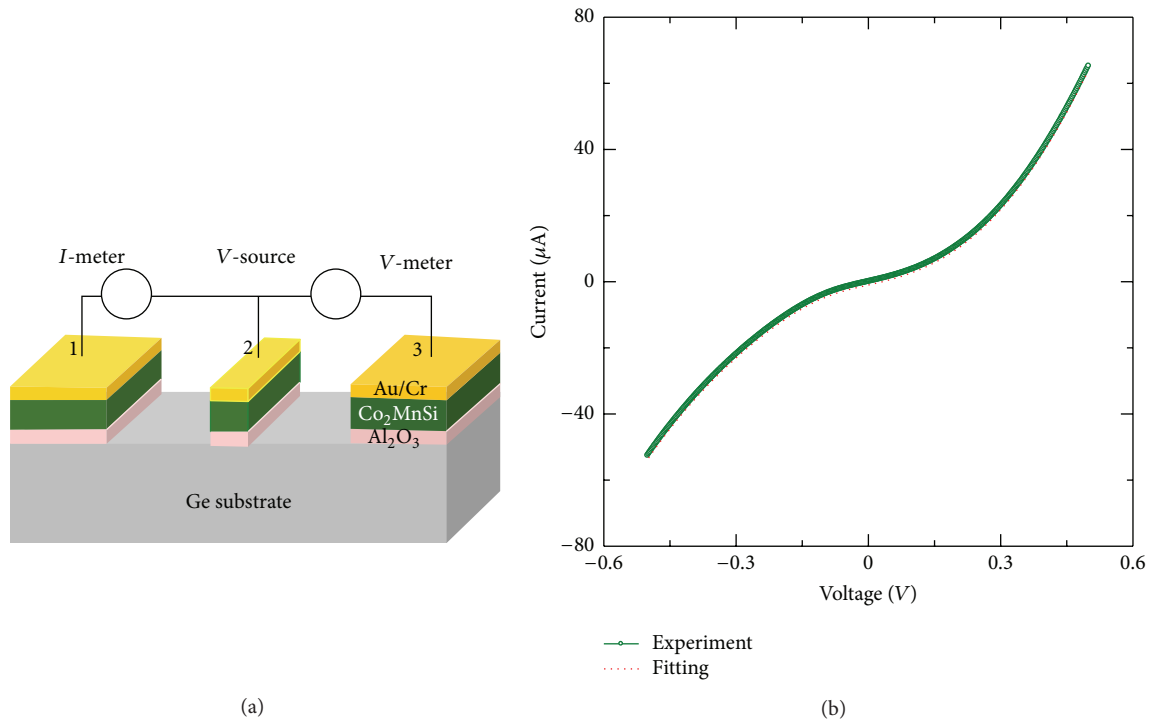


FIGURE 2: (a) A schematic diagram of the device structure and the three-terminal circuit geometry for measuring  $I$ - $V$  characteristics. (b) Typical  $I$ - $V$  characteristics of a  $\text{Co}_2\text{MnSi}/\text{Al}_2\text{O}_3/n\text{-Ge}$  junction having a junction area of  $60 \times 60 \mu\text{m}^2$  together with a fit to Simmon's model (dotted line).

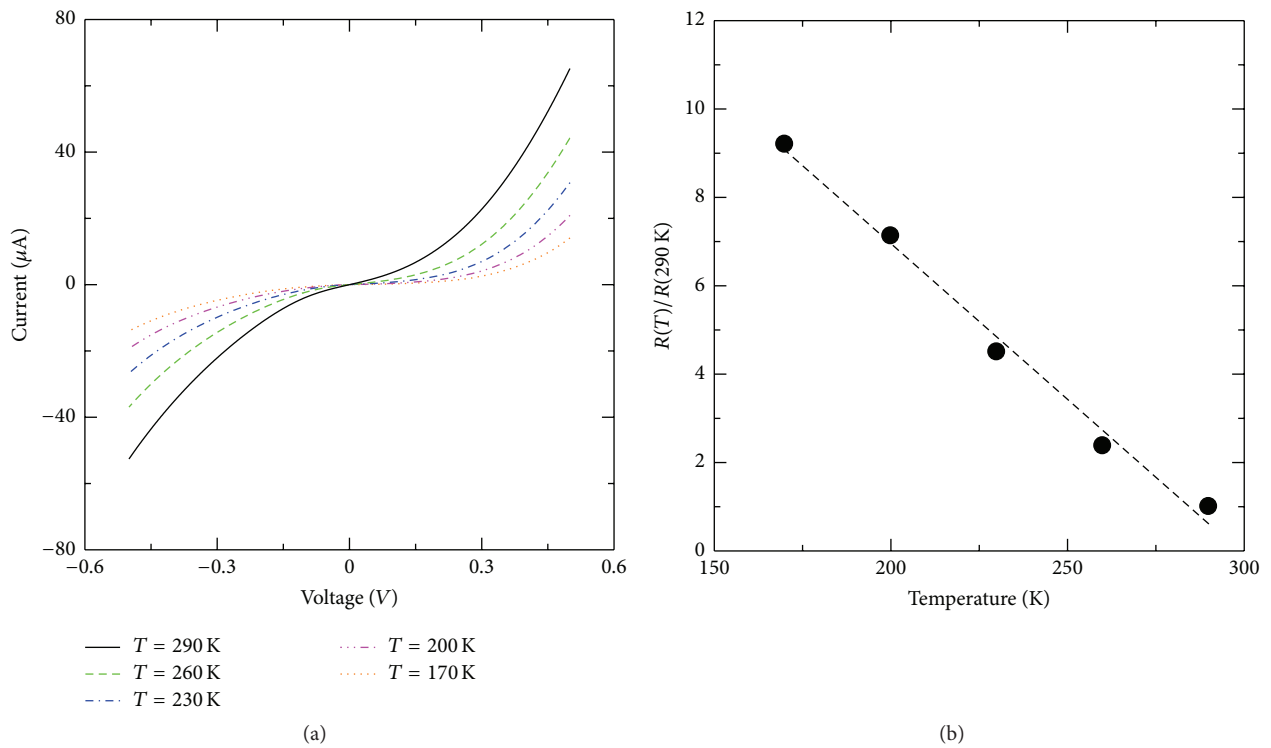


FIGURE 3: (a) Typical  $I$ - $V$  characteristics at various temperatures measured by three-terminal geometry, the junction area was  $60 \times 60 \mu\text{m}^2$ . (b) Different temperature dependence of the ratios of resistance at various temperatures  $T$  and 290 K.

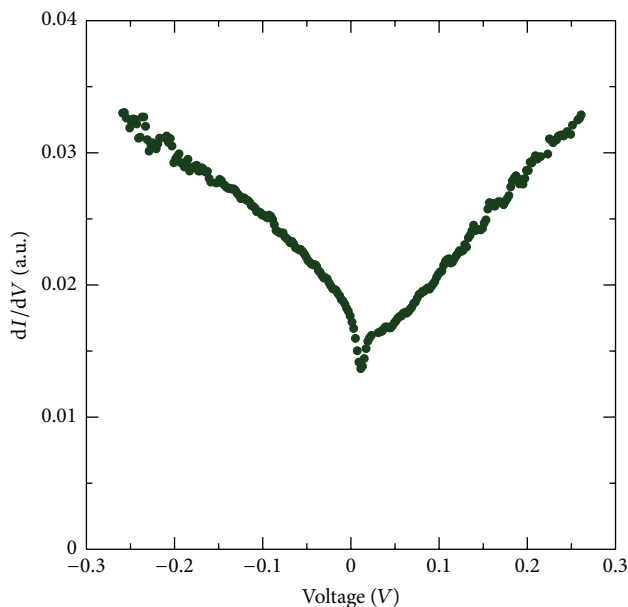


FIGURE 4: Typical conductance versus voltage ( $dI/dV$ - $V$ ) characteristics at 290 K for the  $\text{Co}_2\text{MnSi}/\text{Al}_2\text{O}_3$  (2.0 nm)/ $n$ -Ge heterostructure.

$V$ , a marked increase in conductance was clearly observed with  $|V| > 14$  mV. The  $dI/dV$ - $V$  curve shows a typical signature of tunneling behavior with the applied voltage and the curve is highly symmetric with smaller voltage region. We calculated the potential barrier height and tunnel barrier thickness by the Brinkman-Dynes-Rowell model, and almost the same values were yielded with that fitted by Simmons model.

#### 4. Conclusions

In summary, Heusler alloy  $\text{Co}_2\text{MnSi}$  thin films grown on Ge(001) substrates via an  $\text{Al}_2\text{O}_3$  tunneling barrier were prepared. The sufficiently high saturation magnetization  $781 \text{ emu/cm}^3$  was in good agreement with the  $859 \text{ emu/cm}^3$  for  $\text{Co}_2\text{MnSi}$  thin film grown on the MgO-buffered MgO substrate. Furthermore, the  $I$ - $V$  characteristics showed nonlinear characteristics and were almost symmetric with respect to the bias polarity, indicating that the tunneling conduction was dominant. In addition, the  $I$ - $V$  characteristics were slightly dependent on temperature and we found that  $R(T)/R(290 \text{ K})$  shows a weak dependence on the temperature which was as expected for tunneling characteristics. Moreover, the potential barrier height at the  $\text{Co}_2\text{MnSi}/\text{Al}_2\text{O}_3$  interface was almost equal to that at the  $n$ -Ge/ $\text{Al}_2\text{O}_3$  interface. Third, these results confirmed that  $\text{Co}_2\text{MnSi}/\text{Al}_2\text{O}_3/\text{Ge}(001)$  heterostructure is a promising candidate for spin injection into semiconductor channel.

#### Conflict of Interests

The authors declare that there is no conflict of interests regarding the publication of this paper.

#### Acknowledgments

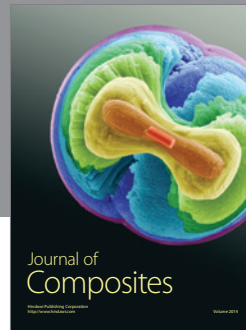
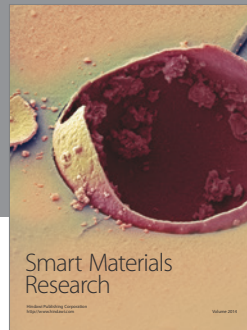
The authors are grateful for the financial support from the National Natural Science Foundation of China (61504107) and Fundamental Research Funds for the Central Universities (3102014JCQ01059 and 3102015ZY043), China.

#### References

- [1] X. Lou, C. Adelman, S. A. Crooker et al., "Electrical detection of spin transport in lateral ferromagnet-semiconductor devices," *Nature Physics*, vol. 3, no. 3, pp. 197–202, 2007.
- [2] S. P. Dash, S. Sharma, R. S. Patel, M. P. de Jong, and R. Jansen, "Electrical creation of spin polarization in silicon at room temperature," *Nature*, vol. 462, no. 7272, pp. 491–494, 2009.
- [3] M. Tran, H. Jaffrès, C. Deranlot et al., "Enhancement of the spin accumulation at the interface between a spin-polarized tunnel junction and a semiconductor," *Physical Review Letters*, vol. 102, no. 3, Article ID 036601, 2009.
- [4] H. Saito, S. Watanabe, Y. Mineno et al., "Electrical creation of spin accumulation in p-type germanium," *Solid State Communications*, vol. 151, no. 17, pp. 1159–1161, 2011.
- [5] A. Jain, L. Louahadj, J. Peiro et al., "Electrical spin injection and detection at  $\text{Al}_2\text{O}_3/n$ -type germanium interface using three terminal geometry," *Applied Physics Letters*, vol. 99, no. 16, Article ID 162102, 2011.
- [6] Y. Zhou, W. Han, L.-T. Chang et al., "Electrical spin injection and transport in germanium," *Physical Review B—Condensed Matter and Materials Physics*, vol. 84, no. 12, Article ID 125323, 2011.
- [7] S. Picozzi, A. Continenza, and A. J. Freeman, " $\text{Co}_2\text{MnX}$  ( $X = \text{Si}, \text{Ge}, \text{Sn}$ ) Heusler compounds: an *ab initio* study of their structural, electronic, and magnetic properties at zero and elevated pressure," *Physical Review B*, vol. 66, no. 9, Article ID 094421, 2002.
- [8] M. Jourdan, J. Minár, J. Braun et al., "Direct observation of half-metallicity in the Heusler compound  $\text{Co}_2\text{MnSi}$ ," *Nature Communications*, vol. 5, article 3974, 2014.
- [9] H.-X. Liu, Y. Honda, T. Taira et al., "Giant tunneling magnetoresistance in epitaxial  $\text{Co}_2\text{MnSi}/\text{MgO}/\text{Co}_2\text{MnSi}$  magnetic tunnel junctions by half-metallicity of  $\text{Co}_2\text{MnSi}$  and coherent tunneling," *Applied Physics Letters*, vol. 101, no. 13, Article ID 132418, 2012.
- [10] G. Schmidt, D. Ferrand, L. W. Molenkamp, A. T. Filip, and B. J. van Wees, "Fundamental obstacle for electrical spin injection from a ferromagnetic metal into a diffusive semiconductor," *Physical Review B*, vol. 62, no. 8, pp. R4790–R4793, 2000.
- [11] E. I. Rashba, "Theory of electrical spin injection: tunnel contacts as a solution of the conductivity mismatch problem," *Physical Review B*, vol. 62, Article ID R16267, 2000.
- [12] A. Fert and H. Jaffrès, "Conditions for efficient spin injection from a ferromagnetic metal into a semiconductor," *Physical Review B*, vol. 64, Article ID 184420, 2001.
- [13] S. Takahashi and S. Maekawa, "Spin injection and detection in magnetic nanostructures," *Physical Review B*, vol. 67, no. 5, Article ID 052409, 2003.
- [14] Y. Song and H. Dery, "Spin transport theory in ferromagnet/semiconductor systems with noncollinear magnetization configurations," *Physical Review B—Condensed Matter and Materials Physics*, vol. 81, no. 4, Article ID 045321, 2010.



- [15] T. Uemura, K. Kondo, J. Fujisawa, K.-I. Matsuda, and M. Yamamoto, "Critical effect of spin-dependent transport in a tunnel barrier on enhanced Hanle-type signals observed in three-terminal geometry," *Applied Physics Letters*, vol. 101, no. 13, Article ID 132411, 2012.
- [16] I. A. Fischer, L.-T. Chang, C. Sürgers et al., "Hanle-effect measurements of spin injection from  $\text{Mn}_5\text{Ge}_3\text{C}_{0.8}/\text{Al}_2\text{O}_3$ -contacts into degenerately doped Ge channels on Si," *Applied Physics Letters*, vol. 105, Article ID 222408, 2014.
- [17] G.-F. Li, T. Taira, K.-I. Matsuda, M. Arita, T. Uemura, and M. Yamamoto, "Epitaxial growth of Heusler alloy  $\text{Co}_2\text{MnSi}/\text{MgO}$  heterostructures on Ge(001) substrates," *Applied Physics Letters*, vol. 98, no. 26, Article ID 262505, 2011.
- [18] H. Kijima, T. Ishikawa, T. Marukame et al., "Epitaxial growth of full-Heusler alloy  $\text{Co}_2\text{MnSi}$  thin films on MgO-buffered MgO substrates," *IEEE Transactions on Magnetics*, vol. 42, no. 10, pp. 2688–2690, 2006.
- [19] J. G. Simmons, "Generalized formula for the electric tunnel effect between similar electrodes separated by a thin insulating film," *Journal of Applied Physics*, vol. 34, no. 6, pp. 1793–1803, 1963.
- [20] S. M. Sze, *Physics of Semiconductor Devices*, Wiley, New York, NY, USA, 1981.



**Hindawi**

Submit your manuscripts at  
<http://www.hindawi.com>

